PHYSICAL REVIEW D **84,** 024012 (2011)

Quasitopological Lifshitz black holes

W. G. Brenna,[1,2,*] M. H. Dehghani,[3,4,†] and R. B. Mann[1,‡]

[1]*Department of Physics & Astronomy, University of Waterloo, 200 University Avenue West, Waterloo, Ontario, Canada N2L 3G1*
[2]*Department of Physics and Engineering Physics, University of Saskatchewan, 116 Science Place, Saskatoon, Saskatchewan S7N 5E2*
[3]*Physics Department and Biruni Observatory, College of Sciences, Shiraz University, Shiraz 71454, Iran*
[4]*Research Institute for Astrophysics and Astronomy of Maragha (RIAAM), Maragha, Iran*
(Received 1 February 2011; published 7 July 2011)

We investigate the effects of including a quasitopological cubic curvature term to the Gauss-Bonnet action to five-dimensional Einstein gravity coupled to a Proca field and search for solutions with asymptotically Lifshitz scaling symmetry. We find that a new set of Lifshitz black hole solutions exist that are analogous to those obtained in third-order Lovelock gravity in higher dimensions. No additional matter fields are required to obtain solutions with asymptotic Lifshitz behavior, though we also investigate solutions with matter. Furthermore, we examine black hole solutions and their thermodynamics in this situation and find that a negative quasitopological term, just like a positive Gauss-Bonnet term, prevents instabilities in what are ordinarily unstable Einsteinian black holes.

DOI: 10.1103/PhysRevD.84.024012 PACS numbers: 04.50.Kd, 04.50.Gh, 04.70.Bw, 04.70.Dy

I. INTRODUCTION

The concept of holography has proven to be enormously fruitful for demonstrating interesting new connections between disparate areas of physics. The basic idea is that gravitational dynamics in a given dimensionality can be mapped onto some other (nongravitational) field theory of a lower dimensionality. Holography has been most thoroughly explored in the context of the AdS/CFT correspondence conjecture, in which a large volume of calculational evidence indicates that a (relativistic) conformal field theory (CFT) can be mapped to gravitational dynamics in an asymptotically anti-de Sitter (AdS) spacetime of one larger dimension [1].

Over the past few years it has become clear that holographic concepts cover a much broader conceptual territory. For example, holographic renormalization has been shown to be a useful tool for understanding conserved quantities and gravitational thermodynamics in both asymptotically de Sitter [2] and asymptotically flat spacetimes [3]. Much more recently holography has been extended to describe a duality between a broad range of strongly coupled field theories and gravity in the context of QCD quark-gluon plasmas [4], atomic physics, and condensed matter physics [5–7].

Gravity-gauge duality is evidently a robust concept, and its full implications for physics (for example, in elucidating the strong coupling behavior of the nongravitational theories noted above) remain to be understood. One line of investigation has been concerned with Lifshitz field theories, which have an anisotropic scaling of the form

$$t \rightarrow \lambda^z t, \qquad r \rightarrow \lambda^{-1} r, \qquad x \rightarrow \lambda x \tag{1}$$

exhibited by fixed points governing the behavior of various condensed matter systems. Such scaling offers some promise for further extending holographic duality between condensed matter physics and gravity. While for $z = 1$ this scaling symmetry is the familiar conformal symmetry, for $z = 3$, theories with this type of scaling are power-counting renormalizable, possibly providing a UV completion to the effective gravitational field theory [8]. For solutions with asymptotically Lifshitz scaling symmetry, the natural spacetime metric is

$$ds^2 = -\frac{r^{2z}}{L^{2z}}dt^2 + L^{-2}\left(\frac{dr^2}{r^2} + r^2 d\Omega^2\right) \tag{2}$$

noted earlier in a braneworld context [9].

A D-dimensional anisotropic scale invariant background using an action that couples gravity to a massive gauge field [or alternatively to 2-form and dualized $(D-1)$-form field strengths with a Chern-Simons coupling] can be constructed that has solutions with the asymptotic behavior (2) [10]. An early example [11] for an extended class of vacuum solutions for a sort of higher-dimensional dilaton gravity with general z was soon followed by the discovery of black hole solutions, both exact (for $z = 2$) [12] and numerical (for more general values of z) [12–15].

Since in general one expects quantum-gravitational effects to induce corrections to the Einstein action, it is natural to consider modifying the gravitational part of the action with higher-derivative terms due to additional powers of the curvature. Such terms must be considered on the gravity side of the duality conjecture in order to study CFTs with different values for their central charges. Here, Lovelock gravity theories play a special role in that the number of metric derivatives in any field equation is never larger than 2. Furthermore, third-order Lovelock gravity is supersymmetric, and therefore one can define

*wgb278@mail.usask.ca
†mhd@shirazu.ac.ir
‡rbmann@sciborg.uwaterloo.ca

superconformal field theories via the AdS/CFT correspondence [16,17].

The addition to the action of a term cubic in curvature is not new, but asymptotic Lifshitz solutions in Lovelock gravity coupled to a massive Abelian gauge field were only recently discovered [18]. For a suitable choice of coupling constant, one can dispense with this massive gauge field, since the additional Lovelock terms can play the role of the desired matter. Some new exact black hole solutions were obtained as well as a broad class of numerical solutions, and asymptotic Lifshitz solutions with curvature-squared terms in the action have also been investigated [19–22]. Somewhat remarkably, the relationship between the energy density, temperature, and entropy density is unchanged from Einsteinian gravity [23] even though the subleading large-r behavior of Lovelock-Lifshitz black branes differs substantively from their Einsteinian Lifshitz counterparts [12,15]. The relationship between entropy and temperature is also the same as the Einsteinian case, apart from a constant of integration that depends on the Lovelock coefficients.

The hallmark feature of Lovelock theories is that no field equation has more than two derivatives of any metric coefficient. However, a new cubic curvature term was recently introduced that can perhaps be regarded as a generalization of Lovelock gravity in five dimensions [24,25]. The generality arises from a spherical symmetry requirement: the field equations will generally reduce to a second-order system of differential equations when the metric is spherically symmetric.

This particular class of correction terms has been coined quasitopological gravity, since in some ways they behave like topological invariants in six dimensions, yet for nonspherical geometries, they contribute nontrivially to the action. Furthermore, there are no Lagrangians that are cubic in curvature in four dimensions for spherical symmetry that lead to second-order differential equations. Quasitopological gravity has been previously studied in the case of planar AdS black holes. In this paper we investigate the implications of this new term for asymptotically Lifshitz spacetimes. We shall refer to this class of solutions as quasitopological Lifshitz solutions.

Specifically, we examine the effects of higher-curvature modifications to Einsteinian gravity to asymptotically Lifshitz metrics, both with and without massive background Abelian gauge fields. We find that the quasitopological field equations replicate those from third-order Lovelock gravity [18], provided the quasitopological parameter μ is appropriately renormalized. We find that indeed, asymptotic Lifshitz black holes exist in both cases. We obtain both exact solutions and numerical ones, the latter obtained via the shooting method. We close with a short discussion of the relevant thermodynamics and conserved quantities of our black hole solutions.

II. QUASITOPOLOGICAL GRAVITY

The quasitopological additions consist of third-order curvature corrections to Gauss-Bonnet gravity that maintain second-order field equations with respect to the metric under conditions of spherical symmetry. We use the action

$$I = \int d^D x\sqrt{-g}\Big(-2\Lambda + \mathcal{L}_1 + \frac{\lambda L^2}{(D-3)(D-4)}\mathcal{L}_2 - \frac{8\mu L^4}{(D-3)(D-6)}\mathcal{L}_3 - \frac{1}{4}F_{\mu\nu}F^{\mu\nu} - \frac{1}{2}m^2 A_\mu A^\mu\Big), \tag{3}$$

where D is the number of dimensions (larger than four and different from six), $F_{\mu\nu} = \partial_{[\mu}A_{\nu]}$, μ and λ are the correction terms' coefficients, $\mathcal{L}_1 = R$ is the Ricci scalar, $\mathcal{L}_2 = R_{\mu\nu\gamma\delta}R^{\mu\nu\gamma\delta} - 4R_{\mu\nu}R^{\mu\nu} + R^2$ is the Gauss-Bonnet Lagrangian, and $\mathcal{L}_3$ is the quasitopological gravity correction. This quasitopological gravity correction has the form

$$\mathcal{L}_3 = \frac{2D-3}{3D^2-15D+16}R_{\mu}{}^{\nu}{}_{\lambda}{}^{\rho}R_{\nu}{}^{\tau}{}_{\rho}{}^{\sigma}R_{\tau}{}^{\mu}{}_{\sigma}{}^{\lambda} + \frac{3}{(D-4)(3D^2-15D+16)}\Big(\frac{3D-8}{8}R_{\mu\lambda\nu\rho}R^{\mu\lambda\nu\rho}R - (D-2)R_{\mu\lambda\nu\rho}R^{\mu\lambda\nu}{}_{\tau}R^{\rho\tau} + DR_{\mu\lambda\nu\rho}R^{\mu\nu}R^{\lambda\rho} + 2(D-2)R_{\mu}{}^{\lambda}R_{\lambda}{}^{\nu}R_{\nu}{}^{\mu} - \frac{3D-4}{2}R_{\mu}{}^{\lambda}R_{\lambda}{}^{\mu}R + \frac{D}{8}R^3\Big). \tag{4}$$

This term is only effective in dimensions greater than four, and it becomes trivial in six dimensions [25].

Rather than write down the full tensorial expression for the field equations, as we are interested only in spherically symmetric solutions we will insert the asymptotically Lifshitz metric,

$$ds^2 = -\frac{r^{2z}}{L^{2z}}f(r)dt^2 + \frac{L^2 dr^2}{r^2 g(r)} + r^2 d\Omega^2, \tag{5}$$

into the action and then functionally vary it, obtaining (after eliminating redundancies) three equations of motion for the two metric functions and the gauge field. Boundary conditions require that $f(r)$ and $g(r)$ asymptotically reach unity. The term $d\Omega^2$ is the metric for a constant curvature hypersurface,

$$d\Omega^2 = d\theta_1{}^2 + k^{-1}\sin^2(\sqrt{k}\theta_1)\Big(d\theta_2{}^2 + \sum_{i=3}^{D-2}\prod_{j=2}^{i-1}\sin^2\theta_j d\theta_i{}^2\Big), \tag{6}$$

where parameter k is either -1, 0, or 1, providing hyperbolic, flat, and spherical geometries, respectively.

For $k = 0$ a coordinate transformation will reduce this to the form $\sum_k^{D-2} d\theta_k{}^2$. Symmetry requirements imply that the gauge field ansatz is

$$A_t = q\frac{r^z}{L^z}h(r), \tag{7}$$

with all other components vanishing.

Now that the formalism has been specified, we restrict our considerations to five dimensions and so (unless otherwise stated) the following results are only valid $D = 5$. Rather than carry out a full variational principle, we insert the ansatz (5) and (7) into the action, obtaining the effective action

$$I = \int d^4x \int dr \frac{r^{z-1}}{kL^{z+1}}\sqrt{\frac{f}{g}}\left(\left\{3r^4\left(\frac{-\Lambda}{6}L^2 - \kappa + \lambda\kappa^2 + \mu\kappa^3\right)\right\}' + \frac{q^2r^3}{2f}(g(rh' + zh)^2 + m^2L^2h^2)\right) \tag{8}$$

for the spherically symmetric case, where $\kappa = (g - \frac{L^2}{r^2}k)$.

Functionally varying (8) with respect to $g(r)$, $f(r)$, and $h(r)$, respectively, yields upon simplification

$$\begin{aligned}&\Lambda L^2r^6 + (3z+3)r^6g - 6z\lambda r^6g^2 + 6z\lambda r^4L^2kg - 3r^4L^2k - (9z-3)\mu r^6g^3 + (18z-9)\mu r^4L^2kg^2\\ &\quad - (9z-9)\mu L^4k^2r^2g - 3\mu L^6k^3 + g(\ln f)'\left(\frac{3}{2}r^7 - 3\lambda r^7g + 3\lambda r^5L^2k - \frac{9}{2}\mu r^7g^2 + 9\mu r^5gL^2k - \frac{9}{2}\mu r^3L^4k^2\right)\\ &\qquad = \frac{q^2r^6}{4f}[g(rh' + zh)^2 - m^2L^2h^2]\end{aligned} \tag{9}$$

$$\left(3r^4\left[-\frac{\Lambda}{6}L^2 - \kappa + \lambda\kappa^2 + \mu\kappa^3\right]\right)' = \frac{q^2r^3}{2f}[g(rh' + zh)^2 + m^2L^2h^2] \tag{10}$$

$$2r^2h'' - r[(\ln f)' - (\ln g)'](rh' + zh) + 2(z+4)rh' + 6zh = 2m^2L^2\frac{h}{g}, \tag{11}$$

where a prime ($'$) represents differentiation with respect to the radial coordinate r.

Before trying to find solutions to the above equations, we present a first integral for the above equations of motion. It is a matter of calculation to show that this conserved quantity can be written as

$$\mathcal{C}_0 = [(1 - 2\lambda g - 3\mu g^2)(rf' + 2(z-1)f) - q^2(zh + rh')h] \times \frac{r^{z+D-2}}{L^{z+1}}\left(\frac{f}{g}\right)^{1/2}, \tag{12}$$

with details of this result given in Appendix A. For $z = 1$, $f(r) = g(r)$ and the constant reduces (in the matter-free case) to

$$\mathcal{C}_0 = \frac{r^D}{L^2}(f - \lambda f^2 - \mu f^3)',$$

which is proportional to the mass of black hole.

III. BLACK HOLES

A. Matter-free solutions

Setting $h(r) = 0$, we first consider the existence of solutions of the form

$$ds^2 = -\frac{r^{2z}}{L^{2z}}dt^2 + \frac{L^2dr^2}{r^2} + r^2\sum_{i=1}^{3}d\theta_i^2, \tag{13}$$

where $k = 0$. This is a Lifshitz analogue of flat space for asymptotically flat solutions, whose properties have been discussed elsewhere [26]. We shall refer to such solutions as “Lifshitz solutions.”

For the metric (13) the field equations (9) and (10) imply

$$\Lambda = -\frac{2}{L^2}(2 - \lambda), \qquad \mu = \frac{1}{3}(1 - 2\lambda), \tag{14}$$

independent of our choice of z. These constraints reduce to those of five-dimensional Gauss-Bonnet gravity [18],

$$\Lambda = -\frac{3}{L^2} \quad \text{and} \quad \lambda = \frac{1}{2}, \tag{15}$$

when $\mu = 0$. Note that the same constraints are necessary to ensure the existence of asymptotic Lifshitz solutions if $k \neq 0$.

With the above constraints, the exact Lifshitz solution [that is, $f(r) = g(r) = 1$] is a solution to the field equations for any value of z. Equation (10) with the condition (14) reduces to

$$2 - \lambda - 3\kappa + 3\lambda\kappa^2 + (1 - 2\lambda)\kappa^3 = \frac{C}{r^4}, \tag{16}$$

where C is a constant of integration. For $C = 0$, $\kappa = 1$ or

$$g(r) = 1 + \frac{kL^2}{r^2} \tag{17}$$

yielding the only solution of Eq. (16) that has the desired asymptotic behavior. The function $f(r)$ is not restricted by Eq. (9). This degeneracy of the field equations has been noted previously in five-dimensional Einstein-Gauss-Bonnet gravity with a cosmological constant [27] and third-order Lovelock gravity [18]. In the Gauss-Bonnet case, it was shown that there exists a degenerate set of solutions where $f(r)$ is left unspecified, while for certain values of the Gauss-Bonnet parameter, $f(r) = g(r)$. In our case, this degeneracy is lifted when matter is present, and we obtain a family of solutions that become unique for a specific field strength, as we shall see.

Choosing $f(r) = g(r)$ (as in Lovelock gravity [18]) yields for $k = -1$ an event horizon, and consequently the metric

$$ds^2 = -\frac{r^{2z}}{L^{2z}}\left(1 - \frac{L^2}{r^2}\right)dt^2 + \frac{L^2 dr^2}{r^2(1 - \frac{L^2}{r^2})} + r^2 d\Omega^2_{-1} \tag{18}$$

which is an exact black hole solution.

For $C \neq 0$, one can find κ and therefore $g(r)$, but upon inserting this solution in Eq. (9), we find that the solution for $f(r)$ does not exhibit the desired asymptotic behavior. We find, with one exception, no other exact solutions to the field equations for these symmetries and asymptotic behavior.

The exception is $z = 1$ (AdS), for which an exact solution can be found. The requirements that $f(r) = g(r)$ and $h(r) = 0$ produce exact solutions dependent on λ if $\mu = 0$ [28]. Setting $\mu \neq 0$, we first seek solutions for $z = 1$ without any background gauge field. Restricting $f(r) = g(r)$ and setting $h(r) = 0$, the field equation (11) disappears, while Eqs. (9) and (10) are not independent and can be analytically solved. The result is

$$\begin{aligned} f(r) &= g(r) \\ &= \frac{kL^2}{r^2} - \frac{\lambda}{3\mu} + \frac{1}{12\mu r^2}\Big[\Big(\sqrt{\Gamma + J^2(r)} + J(r)\Big)^{1/3} \\ &\quad - \Big(\sqrt{\Gamma + J^2(r)} - J(r)\Big)^{1/3}\Big], \end{aligned} \tag{19}$$

where we define

$$\begin{aligned} \Gamma &= -(16r^4(3\mu + \lambda^2))^3 \\ J(r) &= 16r^6\left(4\lambda^3 + 18\mu\lambda - 9\mu^2\Lambda L^2 - 18\frac{M\mu^2}{r^4}\right) \end{aligned} \tag{20}$$

and M is a constant of integration. This solution matches the form of one obtained in third-order Lovelock gravity for $D > 6$ [28], as our field equations are of the same form. With this exact solution, we are able to compare results with the numerical algorithm.

B. Matter solutions

In the presence of a massive gauge field [$h(r) \neq 0$] the Lifshitz solution (13) is also supported by quasitopological gravity provided

$$\begin{aligned} q^2 &= \frac{2(z-1)(1-2\lambda-3\mu)}{z} \qquad m^2 = \frac{3z}{L^2} \\ \Lambda &= -\frac{1}{2L^2}[(1-2\lambda-3\mu)(2z+z^2) + 9 - 6\lambda - 3\mu] \\ &\quad \lambda < \frac{1}{2}(1-3\mu), \end{aligned} \tag{21}$$

where the last constraint arises because we require $q^2 > 0$. This in turn implies

$$\frac{3\mu(z+1)^2 - (z^2+2z+9)}{2L^2} \leq \Lambda \leq -\frac{3}{2L^2}(1+\mu)$$

provided $\lambda > 0$, as is normative for Gauss-Bonnet gravity in the context of heterotic string theory [29].

We look for black hole solutions using both near-horizon and asymptotic series expansions of the metric and gauge functions. The near-horizon series solutions are then used to obtain initial conditions for the numerical solution of the field equations. The restrictions on $f(r)$ and $g(r)$ now become more rigid: these functions must not only approach unity as $r \to \infty$ (to satisfy the asymptotically Lifshitz boundary conditions) but they must also tend towards zero as $r \to r_0$ in order to ensure an event horizon exists. First, we will show that series representations exist near and far from the horizon, and then we present a set of solutions obtained by numerically solving the differential equations (9)–(11).

1. Series solutions

We begin by searching for well-behaved black hole solutions in a near-horizon regime. Our ansatz requires that the metric functions go to zero linearly near the horizon $r = r_0$:

$$\begin{aligned} f(r) &= f_1\{(r-r_0) + f_2(r-r_0)^2 + f_3(r-r_0)^3 + \cdots\}, \\ g(r) &= g_1(r-r_0) + g_2(r-r_0)^2 + g_3(r-r_0)^3 + \cdots, \\ h(r) &= f_1^{1/2}\{h_0 + h_1(r-r_0) + h_2(r-r_0)^2 \\ &\quad + h_3(r-r_0)^3 + \cdots\}, \end{aligned} \tag{22}$$

and we find that the substitution of this ansatz into our equations of motion results in $h_0 = 0$ and a restriction on g_1:

$$\begin{aligned} g_1 = \frac{z}{{r_0}^3}&\{3\mu({r_0}^6(z-1)^2 + 4z{r_0}^6 - 2L^6k^3) \\ &+ 2\lambda{r_0}^6((z+1)^2+2) - {r_0}^4({r_0}^2(z+1)^2 + 8{r_0}^2 + 6L^2k)\} \\ &\times[3\mu((1-z){h_1}^2{r_0}^5 - 3L^4k^2z) + 2\lambda((1-z){r_0}^5{h_1}^2 \\ &+ 3zL^2k{r_0}^2) + ((z-1){h_1}^2{r_0}^5 + 3z{r_0}^4)]^{-1}. \end{aligned} \tag{23}$$

We are left with two free parameters, h_1 and f_1, and values for these are selected to ensure proper asymptotic behavior for large r. All of the other terms in the expansion are solvable in terms of these two parameters.

Solutions at large r can be obtained by linearizing the system, using the ansatz

$$\begin{aligned} f(r) &= 1 + \varepsilon f_e(r), \\ g(r) &= 1 + \varepsilon g_e(r), \\ h(r) &= 1 + \varepsilon h_e(r), \end{aligned} \tag{24}$$

yielding rather lengthy expressions for the leading terms. We have relegated these to Appendix C.

2. Numerical solutions

We will find it easier to obtain numerical solutions by writing

$$\frac{dh}{dr} \equiv j(r), \tag{25}$$

in which case the set of differential equations (9)–(11) can be written as

$$\begin{aligned}
\frac{dj}{dr} &= \frac{zh(3-2g) - z^2hg - rjg(2z+3)}{gr^2} - L_0\frac{r^2h^2(zh+rj)(z-1)}{fgH} \\
\frac{df}{dr} &= \frac{1}{3zr^3gH}\{3[4+6(z-1)]z\mu r^6 fg^3 + 3zr^4[-3k\mu L^2(4z-2) + (4z)\lambda r^2]fg^2 \\
&\quad - 3zr^2[3(2z-2)k^2\mu + 4zk\lambda L^2r^2 + (2z+2)r^4]fg - z\mu\{[3(z-1)^2+12z]r^6 - 6k^3L^6\}f \\
&\quad - z\lambda r^2\{[2(z-1)^2+8z+4]r^4\}f + zr^4\{[(z-1)^2+4z+8]r^2 + 6kL^2\}f + (z-1)L_0r^6[(zh+rj)^2g - 3zh^2]\} \\
\frac{dg}{dr} &= \frac{1}{3zr^3fH}\{12z\mu r^6fg^3 + 3zr^4[-6L^2k\mu + 4\lambda r^2]fg^2 - 3zr^2[4k\lambda L^2r^2 + 4r^4]fg \\
&\quad - z\mu\{[3(z-1)^2+12z]r^6 - 6k^3L^6\}f - z\lambda r^2\{[2(z-1)^2+8z+4]r^4\}f \\
&\quad + zr^4\{[(z-1)^2+4z+8]r^2 + 6kL^2\}f + (z-1)L_0r^6[(zh+rj)^2g + 3zh^2]\},
\end{aligned} \tag{26}$$

where for simplicity we define $L_0 = -1 + 2\lambda + 3\mu$ and $H = r^4 + 2\lambda r^2(kL^2 - r^2g) - 3\mu(kL^2 - r^2g)^2$.

Equations (25) and (26) form a system of four coupled first order ordinary differential equations. With these ordinary differential equations, initial conditions are chosen from the series solution (evaluated just beyond the horizon), and then the shooting method (explained in [12,15]) is used to obtain solutions.

We consider values of μ and λ that guarantee positivity of the energy flux in the dual conformal field theory [30] when $z = 1$. For $z \neq 1$ the dual theory is not well understood and the analogous allowed ranges of μ and λ are not known. Furthermore, microscopic constraints such as positivity of energy and causality are not necessarily responsible for setting the lower bound on the ratio of shear viscosity to entropy density in the plasma, since hydrodynamic transport is determined by the infrared properties of the system, which do not necessarily enter into the microcausality analysis of the theory [31]. However, for the most part we shall employ the same values of μ and λ as for the $z = 1$ case, noting departures from these values for illustrative purposes as appropriate.

The specific case $z = 1$ eliminates the charge q, and the solution is given by Eq. (19) with $f(r) = g(r)$. Solving the system (9)–(11) yields numerical solutions.

We can check the validity of our numerical approach by comparing this to the exact solution in Eq. (19). For example, for $r_0 = 0.9$, and $k = 0$ we see from Fig. 1 that the two curves (numerical and analytic) are coincident. To be certain, we tested equality of the two approaches for $\mu = -0.001$, $\lambda = 0.04$, $k = 0$, and $r_0 = 1.5$. Evaluating between $r = 1.51$ and $r = 15$ at intervals of 0.01, we find that the two solutions differ by no more than 10^{-7}.

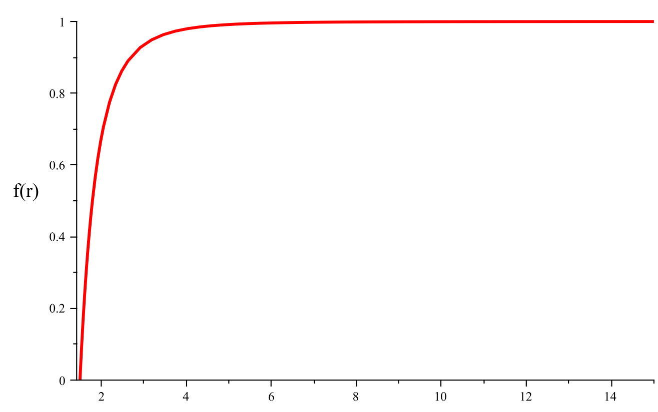

FIG. 1 (color online). Comparison of analytic versus numerical solution for $f(r)$, where $r_0 = 0.9$, $\lambda = 0.04$, $\mu = -0.001$, and $k = 0$. The two curves are identical to one part in 10^{-7}.

For $z \neq 1$, we numerically obtain solutions for large, medium, and small values of r_0 over a broad range of initial values of the field strength (h_1). The quantity f_1 is then fixed by asymptotic conditions. For a given value of h_1, we find that large black holes are asymptotic to functions that monotonically tend to unity, whereas the metric functions for small black holes exhibit a spike in magnitude before settling down. However, due to the extra degree of freedom in the gauge field strength, we can obtain a family of solutions (and control the spike) by varying h_1, subsequently adjusting f_1 to satisfy the asymptotic conditions. In Fig. 2, we see the result of varying the initial value of h_1 from 2.6 (dashed solution) to 2.8 (solid solution). For these the initial values of f_1 remained constant at 2.0. Note that the initial spike present for $h_1 = 2.6$ vanishes for $h_1 = 2.8$.

In Fig. 3, we plot the metric and gauge functions for a large black hole. All three functions monotonically increase from zero at the horizon to unity for large r. Within numerical precision the convergence to unity can be arbitrarily controlled; our plots were produced with convergence of at least one part in 10^{-7}. This convergence to unity takes place for all metric functions we have calculated; we shall omit the large-r behavior of the metric and gauge functions in all subsequent diagrams and illustrate their behavior only for small and medium values of r.

Figure 4 shows a medium black hole ($r_0 = 2.4$), where the dashed line is Einsteinian gravity and the dotted line is quasitopological gravity. Here, due to the more favorable scale, we see that the solution for $h(r)$ is noticeably different. The scale is still too large to see any effect on the $g(r)$ solution, however.

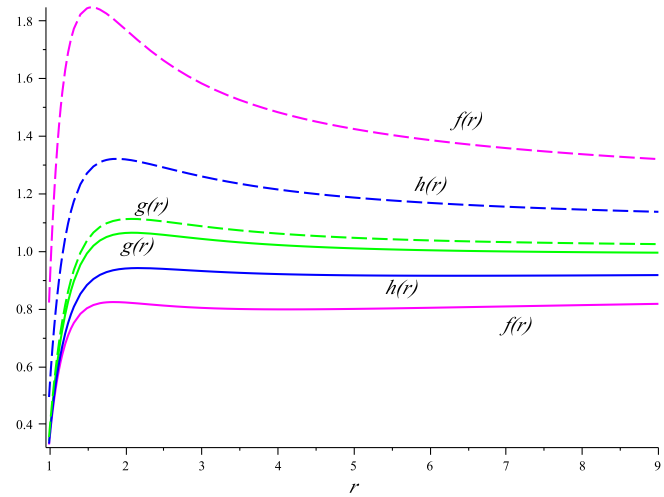

FIG. 2 (color online). Comparison of two sets of $z = 2$ solutions for $h_1 = 2.6$ (dashed) and $h_1 = 2.8$ (solid) for $\lambda = 0.1$ and $\mu = 0.001$, where $f(r)$, $g(r)$, $h(r)$ are plotted versus r respectively in magenta, green, and blue.

We can see from Fig. 5 that for small black holes, $f(r)$ spikes sharply. The plot shows a comparison between Einsteinian gravity (dashed), Gauss-Bonnet gravity (solid), and quasitopological gravity (dotted) for $k = -1$. Small black holes for $k = 0$ and $k = 1$ exhibit similar behavior.

The plot in Fig. 6 better shows the effect of larger values of μ and λ, elucidating how the quasitopological term really affects solutions.

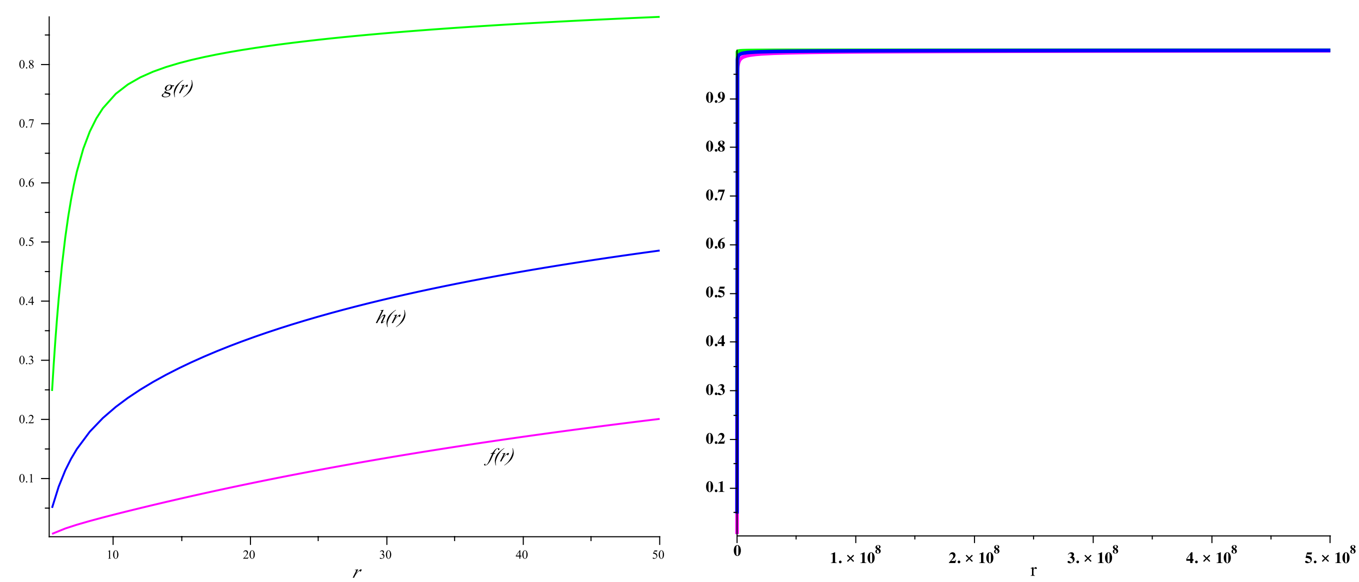

FIG. 3 (color online). Large black hole ($k = 1$) of $r_0 = 5.0$, where $\lambda = 0.04$ and $\mu = -0.001$, with $f(r)$, $g(r)$, $h(r)$ versus r respectively in magenta, green, and blue for $z = 2$. The left/right figures show the behavior for small/large values of r to demonstrate the convergence to unity; note that all three functions are barely distinguishable at the large distance scale.

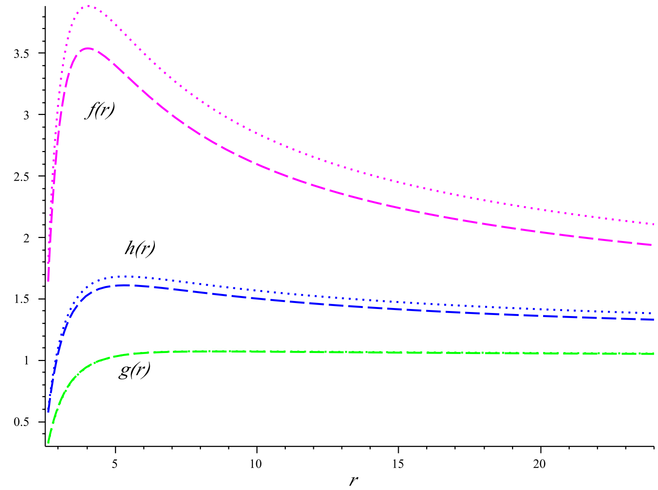

FIG. 4 (color online). Medium black hole of radius $r_0 = 2.4$ ($k = 0$); here $\lambda = 0.04$ and $\mu = -0.001$, and $f(r)$, $g(r)$, $h(r)$ versus r for $z = 2$ respectively in magenta, green, and blue. The dotted line is Einsteinian gravity and the solid line is quasitopological gravity.

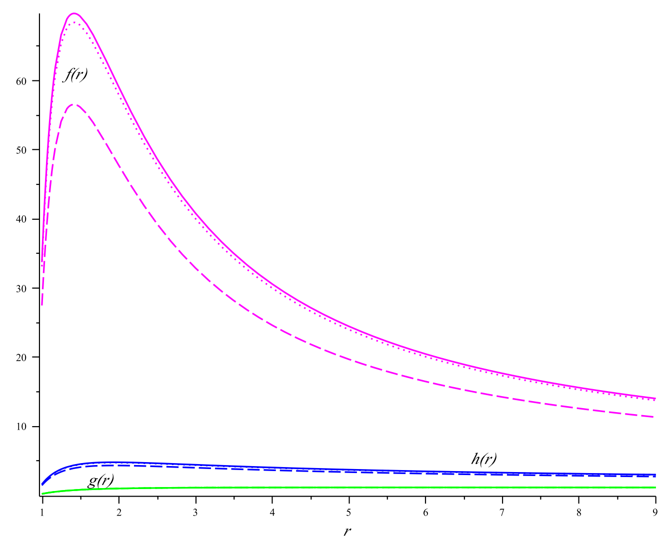

FIG. 5 (color online). Small black hole $r_0 = 0.9$ ($k = -1$), where $\lambda = 0.04$ and $\mu = -0.001$, with $f(r)$, $g(r)$, $h(r)$ versus r for $z = 2$ respectively in magenta, green, and blue for Einsteinian gravity (dashed), Gauss-Bonnet gravity (solid), and quasitopological gravity (dotted).

IV. THERMODYNAMICS

In this section we generalize from five to D dimensions to study the thermodynamic behavior of the solutions we obtain. The Iyer/Wald prescription for black hole entropy is [32,33]

$$S = -2\pi \oint d^{D-2}x\sqrt{\tilde{g}}Y^{abcd}\hat{\epsilon}_{ab}\hat{\epsilon}_{cd}, \quad \text{where } Y^{abcd} = \frac{\partial \mathcal{L}}{\partial R_{abcd}}, \tag{27}$$

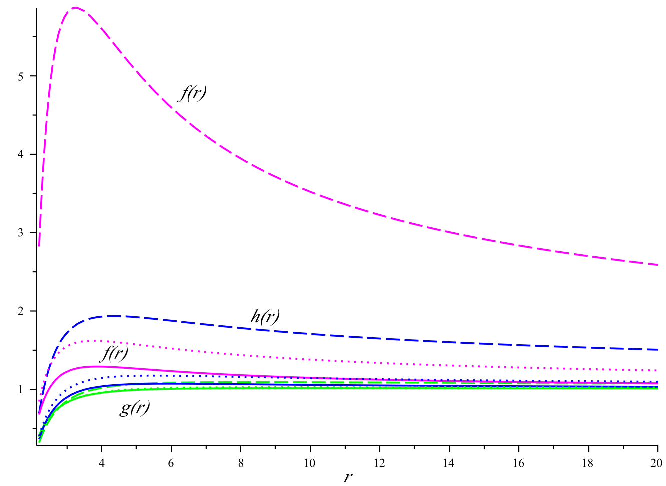

FIG. 6 (color online). Medium $z = 2$ black hole ($r_0 = 2$) with $\mu = 2.5$ and $\lambda = -10$ for $k = -1$ where Einsteinian gravity is solid, Gauss-Bonnet gravity is dashed, and quasitopological gravity is dotted. Similar to above, $f(r)$, $g(r)$, $h(r)$ are magenta, green, and blue.

where $\hat{\epsilon}_{ab}$ is the binormal to the horizon and $\mathcal{L}$ is the Lagrangian, with Latin indices denoting quantities projected onto the horizon surface. For the static black holes considered here, $Y = Y^{abcd}\hat{\epsilon}_{ab}\hat{\epsilon}_{cd}$ is constant on the horizon and so the entropy is given simply as

$$S = -2\pi Y \int d^{D-2}x\sqrt{\tilde{g}}, \tag{28}$$

where the integration is done on the $(D-2)$-dimensional spacelike hypersurface of the Killing horizon with induced metric $\tilde{g}_{ab}$ (whose determinant is $\tilde{g}$). Although the asymptotic behavior of our solution is different from Ref. [25] and $f(r) \neq g(r)$, we obtain the same result:

$$S_k = \frac{A}{4G_D}\left(1 + \frac{2(D-2)}{D-4}\lambda k\frac{L^2}{r_0^2} - \frac{3(D-2)}{D-6}\mu k^2\frac{L^4}{r_0^4}\right), \tag{29}$$

where D is the number of dimensions and A is the surface area of the black hole (since our metric is spherically symmetric, the surface area will be proportional to r_0^{D-2}).

The temperature of the black holes is found by ensuring regularity at the horizon after Wick rotation; we obtain

$$T = \left(\frac{r^{z+1}\sqrt{f'g'}}{4\pi L^{z+1}}\right)_{r=r_0}. \tag{30}$$

This quantity can be numerically calculated, and plotted against entropy on a logarithmic scale, to study stability of the black holes. A negative slope indicates that the black hole will not be in thermal equilibrium and so must decay.

A. Stability of AdS black holes

Plotting the solution for $z = 1$ in five dimensions, which can be checked with the analytic case, we obtain Fig. 7, where we use $\lambda = 0.4$ and $\mu = -0.001$. The solid line is quasitopological gravity, while dots correspond to Gauss-Bonnet and crosses are Einsteinian. The parameter k varies between -1, 0, 1, colored green, blue, and magenta, respectively. Up to the black hole sizes for which we are able to find valid numerical solutions, we see no evidence of unstable black holes for any value of k. In the Einsteinian case we see that small black holes will become unstable for $k = 1$, so it is expected that for sufficiently small values of λ and μ, the solution will be one of small, unstable black holes.

To see what effect the sign of the quasitopological parameter has on black hole stability, we plotted a similar set of curves for a positive value of $\mu = 0.001$. This plot is shown in Fig. 8. We see that for $k = +1$ sufficiently small black holes are thermodynamically unstable.

B. Stability of quasitopological Lifshitz black holes

For $z = 2$, we also plot $\log(T)$ versus $\log(S)$ in Figs. 9 and 10. Note that these plots are also specific to the five-dimensional case. For large black holes, it appears that by varying z we do not change the temperature-entropy relationship, but instead merely introduce a scaling factor to both entropy and temperature terms. It is also apparent that in both cases, positive Gauss-Bonnet and quasitopological terms will both introduce an instability in $k = +1$ black hole solutions. We find that a sufficiently negative quasitopological term partly counteracts the positive Gauss-Bonnet term in Fig. 9. Exploring larger positive and negative values of μ we find that sufficiently large values of $|\mu|$ can produce stable black holes, whereas we obtain unstable $k = 1$ black holes for sufficiently small values of $|\mu|$.

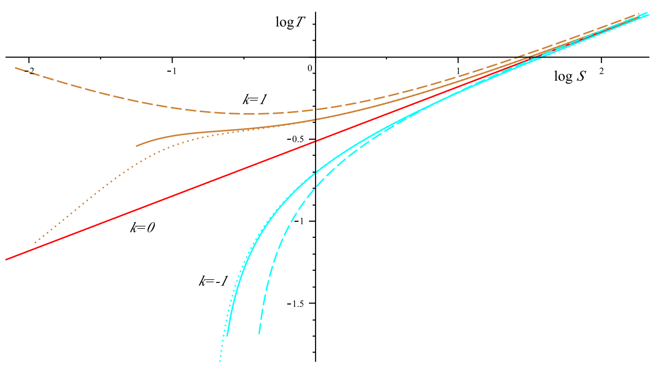

FIG. 7 (color online). $\log(T)$ versus $\log(S)$ for $z = 1$, $\lambda = 0.04$, and $\mu = -0.001$. The solid line is quasitopological gravity, the dotted Gauss-Bonnet, and the dashed Einsteinian. The parameter k varies between -1, 0, 1, colored turquoise, red, and brown, respectively.

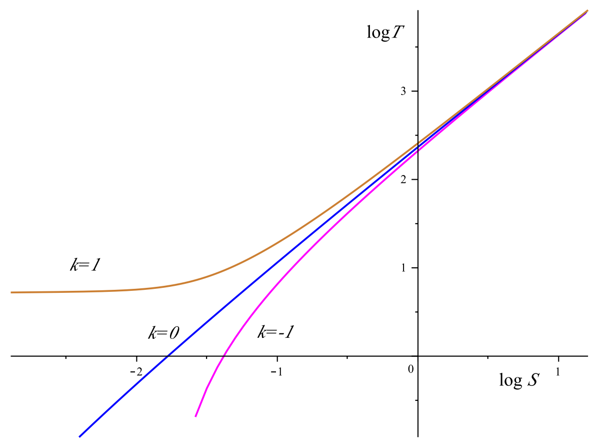

FIG. 9 (color online). $\log(T)$ versus $\log(S)$ for $z = 2$, $\lambda = 0.04$, and $\mu = -0.001$. The parameter k varies between -1, 0, 1, colored magenta, blue, and brown, respectively.

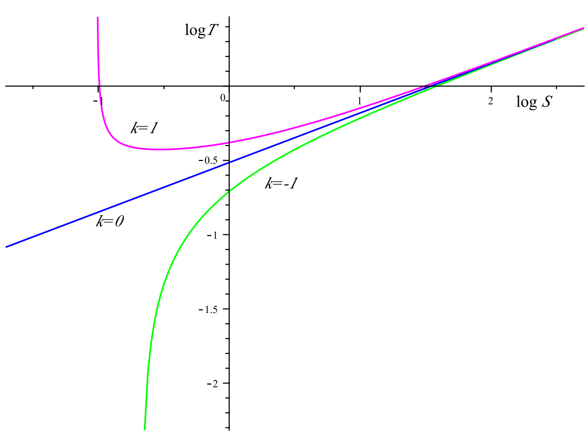

FIG. 8 (color online). $\log(T)$ versus $\log(S)$ for $z = 1$, $\lambda = 0.04$, and $\mu = 0.001$. The parameter k varies between -1, 0, 1, colored green, blue, and magenta, respectively.

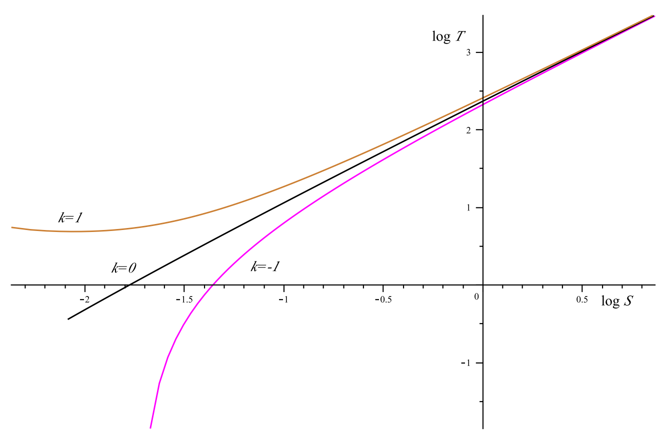

FIG. 10 (color online). $\log(T)$ versus $\log(S)$ for $z = 2$, $\lambda = 0.04$, and $\mu = -0.0003$. The parameter k varies between -1, 0, 1, colored magenta, black, and brown, respectively.

V. CONCLUSIONS

It is well known that the third-order Lovelock term (cubic in the Riemann tensor) does not appear in the field equations in five dimensions as it is a topological invariant. Terms cubic in curvature in general yield higher-order differential equations for metric components. Quasitopological gravity [25] is an exception to this general rule—the cubic terms conspire to yield second-order differential equations for spherically symmetric metrics.

The main result of our paper is to demonstrate that a broad class of solutions—those that are asymptotically Lifshitz—exist in quasitopological gravity in five dimensions. We obtain a family of solutions dependent on two parameters, one giving a measure of the gauge field strength and the other the black hole radius. For a given value of the gauge field strength, we found that there exists a unique solution with asymptotic Lifshitz behavior. Varying the gauge field strength, we found that there exists a family of solutions for a given black hole radius. The r dependence of these solutions varies considerably: the metric functions can develop a "spike" by increasing the gauge field strength. We also find that in general, the quasitopological term acts similarly to the Gauss-Bonnet term, but with opposite sign. When a negative Gauss-Bonnet term decreases the magnitude of the spike, a positive quasitopological term will have the same effect. We see this when a positive quasitopological parameter is added to a Gauss-Bonnet solution that has decreased the magnitude of an Einsteinian spike in $g(r)$: our quasitopological parameter further decreases the magnitude of the spike.

We also investigated the thermal stability of these quasitopological Lifshitz black holes. We found that a negative quasitopological term, just like a positive Gauss-Bonnet term, will prevent instabilities in what are ordinarily unstable Einsteinian black holes. For the asymptotically AdS case ($z = 1$), we found that for sufficiently negative values of μ the instabilities that arise in Einsteinian gravity may be removed, in the same way that a sufficiently positive Gauss-Bonnet term removes the small-r black hole instability. The AdS solutions were seen to be unstable for positive values of μ. With regard to the stability of asymptotically Lifshitz solutions with $z = 2$ in Einstein gravity [12], we found that the quasitopological term can remove instabilities provided the coefficient μ is of sufficient magnitude. Of course, a full stability study would involve a thorough examination of the parameter range for λ and μ.

It is clear that there is much to explore in quasitopological gravity with its addition of new higher-order curvature corrections. The implications of these corrections for the dual theory remain an interesting subject for future investigation.

ACKNOWLEDGMENTS

This work was supported by the Natural Sciences and Engineering Research Council of Canada and Research Institute for Astrophysics and Astronomy of Maragha.

APPENDIX A: THE CONSERVED QUANTITY ALONG THE RADIAL COORDINATE r

In this Appendix, we demonstrate the existence of a constant $\mathcal{C}_0$, which conserved along the radial coordinate r, and compute its form. Since there is no exact quasitopological-Lifshitz solution (except under special circumstances), we calculate it at the horizon and at infinity.

Reparametrizing the metric with the relations

$$\begin{aligned} F(r) &= \frac{1}{2}\ln f(r) + z\ln\frac{r}{L}, \\ G(r) &= -\frac{1}{2}\ln g(r) - \ln\frac{r}{L}, \\ R(r) &= \ln\frac{r}{L}, \\ H(r) &= \ln h(r) + z\ln\frac{r}{L}, \end{aligned} \tag{A1}$$

the metric becomes

$$ds^2 = -e^{2F(r)}dt^2 + e^{2G(r)}dr^2 + e^{2R(r)}\frac{1}{L^2}d\Omega^2 \tag{A2}$$

whose form we insert into the action. Following a similar method to Ref. [23], we integrate by parts and obtain a one-dimensional Lagrangian $\mathcal{L}_{1D} = \mathcal{L}_{1g} + \mathcal{L}_{1m}$ as

$$\begin{aligned} \mathcal{L}_{1g} &= (D-2)\Big(-2\frac{\Lambda}{D-2}e^{2G} + [2F'R' + (D-2)R'^2] \\ &\quad - \frac{\lambda L^2}{3}[4F'R'^3 + (D-5)R'^4]e^{-2G} \\ &\quad - \frac{\mu}{5}L^4[6F'R'^5 + (D-7)R'^6]e^{-4G}\Big)e^{F-G+(D-2)R} \\ \mathcal{L}_{1m} &= \frac{1}{2}q^2(m^2 + H'^2e^{-2G})e^{-F+G+(D-2)R+2H}. \end{aligned} \tag{A3}$$

We are then able to write the equations of motion in the same manner as [23], obtaining the conserved quantity

$$\begin{aligned} \mathcal{C}_0 &= 2(F'-R')(1 - 2\lambda L^2R'^2e^{-2G} \\ &\quad - 3\mu L^4R'^4e^{-4G})e^{F-G+(D-2)R} \\ &\quad - q^2H'e^{-F-G+(D-2)R+2H} \\ &= [(1 - 2\lambda g - 3\mu g^2)(rf' + 2(z-1)f) \\ &\quad - q^2(zh + rh')h]\frac{r^{z+D-2}}{L^{z+1}}\left(\frac{f}{g}\right)^{1/2}. \end{aligned} \tag{A4}$$

This derivation was performed using the form of the quasitopological Lagrangian for D dimensions, given by (4), and the form of the conserved quantity was checked explicitly for D from 7 through 11 to determine the dimensionally independent form given. For any value of z, this conserved quantity arises from the symmetry

$$\begin{pmatrix} F(r) \\ R(r) \\ G(r) \\ H(r) \end{pmatrix} \rightarrow \begin{pmatrix} F(r)+\delta \\ R(r)-\frac{\delta}{D-2} \\ G(r) \\ H(r)+\delta \end{pmatrix}. \tag{A5}$$

For $z=1$, $f(r)=g(r)$ and the constant reduces to

$$\mathcal{C}_0 = \frac{r^D}{L^2}(f-\lambda f^2-\mu f^3)'.$$

APPENDIX B: NEAR-HORIZON SERIES SOLUTION COEFFICIENTS

Here we write down the remaining coefficients of the near-horizon series solution (22) up to second order. Defining for simplicity $L_0=-1+2\lambda+3\mu$, we obtain

$$\begin{aligned} f_2 = {} & \bigg(-6g_1r_0{}^8\bigg(z\bigg(\lambda g_1-\frac{2}{3}h_1{}^2L_0\bigg)+\frac{2}{3}h_1{}^2L_0\bigg)+12zr_0{}^7\bigg(z\bigg(g_1+\frac{1}{2}L_0h_1{}^2\bigg)+\frac{3}{4}g_1-\frac{1}{4}L_0h_1{}^2\bigg) \\ & +18zr_0{}^6\bigg(\frac{1}{9}L_0z^2+\frac{2}{9}L_0z+\frac{1}{3}L_0+\mu L^2kg_1{}^2\bigg)+24kL^2g_1\lambda zr_0{}^5\bigg(z-\frac{1}{4}\bigg) \\ & -36k^2L^4g_1z\mu r_0{}^3\bigg(z-\frac{5}{4}\bigg)+24z\mu L^6k^3\bigg)(r_0(L_0h_1{}^2g_1r_0{}^8-9zr_0{}^7g_1-zr_0{}^6(L_0z^2+2L_0z+3\mu+6\lambda-9) \\ & -18z\lambda L^2kg_1r_0{}^5+6zL^2kr_0{}^4+27L^4k^2\mu zr_0{}^3g_1+6z\mu L^6k^3))^{-1} \end{aligned}$$

$$\begin{aligned} g_2 = {} & (2g_1r_0{}^{12}(L_0(g_1+h_1{}^2(z^2+1)L_0)+z(-3g_1{}^2\lambda-2h_1{}^2g_1L_0-2h_1{}^4L_0{}^2))-3zg_1r_0{}^{11}(z(2g_1+5L_0h_1{}^2) \\ & -13g_1+5h_1{}^2L_0)+r_0{}^{10}(-2z^4L_0(g_1+h_1{}^2L_0)+2z^3L_0(2g_1-h_1{}^2L_0)+z^2(4L_0L^2k\lambda h_1{}^2g_1{}^2+g_1(42\mu+20\lambda+2) \\ & +2h_1{}^2L_0(3\mu-2\lambda+7))+z(6g_1{}^3L^2k(3\mu-2\lambda^2)-8L^2k\lambda h_1{}^2g_1{}^2L_0+g_1(24\mu+48\lambda-72) \\ & +6h_1{}^2L_0(\mu+2\lambda-3))+4L^2k\lambda h_1{}^2g_1{}^2L_0)-6L^2kzg_1\lambda r_0{}^9(z(4g_1+5h_1{}^2L_0)-22g_1+5h_1{}^2) \\ & -4L^2kr_0{}^8\bigg(z^4\lambda g_1L_0-2z^3\lambda g_1L_0+z^2\bigg(\frac{3}{2}\mu L^2kh_1{}^2g_1{}^2L_0+g_1(-3-\lambda-10\lambda^2-21\lambda\mu)-3h_1{}^2L_0\bigg) \\ & +z\bigg(-\frac{27}{2}kL^2g_1{}^3\lambda\mu-3L_0\mu L^2kh_1{}^2g_1{}^2+3g_1(-8\lambda^2-4\mu\lambda+12\lambda+3)+3h_1{}^2L_0\bigg)+\frac{3}{2}L_0\mu L^2kh_1{}^2g_1{}^2\bigg) \\ & +9L^4zk^2g_1r_0{}^7\bigg(z\bigg(g_1\bigg(4\mu-\frac{8}{3}\lambda^2\bigg)+5\mu h_1{}^2L_0\bigg)+g_1(-18\mu+12\lambda^2)-5\mu h_1{}^2L_0\bigg) \\ & +6L^4zk^2g_1r_0{}^6(z^3\mu L_0-2z^2\mu L_0+z(-21\mu^2-\mu-10\lambda\mu+4\lambda)-9kL^2\mu^2g_1{}^2-12\mu^2+\mu(36-24\lambda)-12\lambda) \\ & +36\mu L^6zk^3g_1{}^2\lambda r_0{}^5(2z-7)-12\mu L^6zk^3r_0{}^4(z(2g_1-L_0h_1{}^2)-8g_1+h_1{}^2L_0)+27\mu^2L^8zk^4g_1{}^2r_0{}^3(2z-5) \\ & +24zg_1\mu L^8k^4\lambda r_0{}^2(z-1)-36zg_1\mu^2L^10k^5(z-1))(r_0(-r_0{}^4-2\lambda L^2kr_0{}^2+3L^4k^2\mu)(-L_0g_1(z-1)h_1{}^2r_0{}^8 \\ & +9zg_1r_0{}^7+zr_0{}^6(z^2L_0+2zL_0+3\mu-9+6\lambda)+18z\lambda L^2kg_1r_0{}^5-6zL^2kr_0{}^4-27L^4k^2\mu zr_0{}^3g_1-6z\mu L^6k^3))^{-1} \end{aligned}$$

$$\begin{aligned} h_2 = {} & -h_1(r_0{}^5(z(-2g_1-h_1{}^2L_0)-3g_1+h_1{}^2L_0)+3zr_0{}^4-4L^2kg_1\lambda r_0{}^3(2z+3)+6z\lambda L^2kr_0{}^2+3\mu L^4k^2g_1r_0(2z+3) \\ & -9L^4k^2\mu z)(r_0{}^2g_1(-2r_0{}^4-4\lambda L^2kr_0{}^2+6L^4k^2\mu))^{-1}, \end{aligned}$$

where g_1 is given by (23). Each coefficient depends on the independent parameters r_0 (the horizon radius) and h_1 (proportional to the field strength at the horizon).

APPENDIX C: LARGE r SERIES SOLUTIONS

For large distances away from the black hole, $r \gg L$, we present here series solutions for five dimensions. Considering first the ansatz in (24) for $k=0$, the field equations to first order in ε imply

$$\begin{aligned} 0 &= 2r^2h_e{}''+2rh_e{}'(z+4)+zr(g_e{}'-f_e{}')+6zg_e \\ 0 &= 2r(z-1)h_e{}'+3rg_e{}'+(z^2-z+12)g_e+(z+3)(z-1)(2h_e-f_e) \\ 0 &= 2r(z-1)h_e{}'+3rf_e{}'+\bigg(z^2+\frac{51\mu+22\lambda-5}{3\mu+2\lambda-1}z-18\mu-6\bigg)g_e+(z-3)(z-1)(2h_e-f_e). \end{aligned}$$

The solutions for $f_e(r)$, $g_e(r)$, and $h_e(r)$ yield integer powers of r in a number of special cases. For $h_e(r)$, we find

$$h_e(r) = C_1 r^{-3-z} + r^{(-3-z)/2}(C_2 r^{-\gamma/2} + C_3 r^{\gamma/2}) \tag{C1}$$

$$f_e(r) = \mathcal{D}_1 r^{-3-z} + \mathcal{K} r^{(-3-z)/2}(\mathcal{D}_2 r^{-\gamma/2} + \mathcal{D}_3 r^{\gamma/2}) \tag{C2}$$

$$g_e(r) = \mathcal{F}_1 r^{-3-z} + \mathcal{K} r^{(-3-z)/2}(\mathcal{F}_2 r^{-\gamma/2} + \mathcal{F}_3 r^{-\gamma/2}), \tag{C3}$$

where C_1, C_2, and C_3 are integration constants, L_0 is defined as in Appendix B, and

$$\gamma^2 = \{(-21\mu + 2\lambda - 9)z^2 + (18\mu - 20\lambda + 26)z + 51\mu + 50\lambda - 33\}(-1 + 3\mu + 2\lambda)^{-1}$$
$$\mathcal{D}_1 = C_1 \frac{2L_0(z-3)(z-1)}{2L_0 z^2 - (1 + 6\lambda + 21\mu)z - (9 + 6\lambda + 45\mu)}$$
$$\mathcal{D}_2 = C_2(\mathcal{L}_1 + \mathcal{L}_2)$$
$$\mathcal{D}_3 = C_3(\mathcal{L}_1 - \mathcal{L}_2)$$
$$\mathcal{F}_1 = C_1 \frac{2L_0(z+3)(z-1)}{2L_0 z^2 - (1 + 6\lambda + 21\mu)z - (9 + 6\lambda + 45\mu)}$$
$$\mathcal{F}_2 = C_2(\mathcal{L}_3 + \mathcal{L}_4)$$
$$\mathcal{F}_3 = C_3(\mathcal{L}_3 - \mathcal{L}_4)$$
$$\mathcal{L}_1 = ((1 - 8\lambda - 21\mu)z + 2 + 2\lambda + 12\mu)((36\lambda^2 + (132\mu - 28)\lambda + 9 - 30\mu + 153\mu^2)z^2 + (-40\lambda^2 + (-72\mu + 56)\lambda + 12\mu - 90\mu^2 - 26)z + 68\lambda^2 + (-92 + 132\mu)\lambda - 78\mu + 33 + 81\mu^2)^{1/2}$$
$$\mathcal{L}_2 = (-8\lambda^2 + (-10 - 78\mu)\lambda - 153\mu^2 - 24\mu + 1)z^2 + (20\lambda^2 + (132\mu + 4)\lambda + 5 + 261\mu^2 + 42\mu)z + 6(6\lambda + 15\mu - 1)(\lambda - 1)$$
$$\mathcal{L}_3 = (z-1)L_0((36\lambda^2 + (132\mu - 28)\lambda + 9 - 30\mu + 153\mu^2)z^2 + (-40\lambda^2 + (-72\mu + 56)\lambda + 12\mu - 90\mu^2 - 26)z + 68\lambda^2 + (-92 + 132\mu)\lambda - 78\mu + 33 + 81\mu^2)^{1/2}$$
$$\mathcal{L}_4 = (z-1)L_0((-1 - 6\lambda - 21\mu)z - 3\mu - 10\lambda + 9)$$
$$\mathcal{K} = \frac{1}{2z(12z\mu - z + 5z\lambda + \lambda - 2 - 3\mu)L_0}.$$

For $k = \pm 1$, we can represent the asymptote functions as series

$$f(r) = 1 + \sum_{i=1}^{2(n+z)-3} \frac{a_i}{r^i}$$
$$g(r) = 1 + \sum_{i=1}^{2(n+z)-3} \frac{b_i}{r^i}$$
$$h(r) = 1 + \sum_{i=1}^{2(n+z)-3} \frac{c_i}{r^i}.$$

The coefficients can be determined from direct calculation. Because of the equivalence of our field equations, they match the values obtained in third-order Lovelock gravity [18], once the substitutions $\mu L^4 = -\hat{\alpha}_3$ and $\lambda L^2 = \hat{\alpha}_2$ are made.

For $z = 2$, we obtain nonzero coefficients only for the powers r^{-2}, r^{-5}, r^{-7}, r^{-9}. Just as in Lovelock gravity, at $z = 2$, all of the even powers of r until r^{-5} are present in the large r expansion of the asymptote functions.

[1] J. M. Maldacena, Adv. Theor. Math. Phys. **2**, 231 (1998); Int. J. Theor. Phys. **38**, 1113 (1999); S. S. Gubser, I. R. Klebanov, and A. M. Polyakov, Phys. Lett. B **428**, 105 (1998); E. Witten, Adv. Theor. Math. Phys. **2**, 253 (1998).
[2] A. Strominger, J. High Energy Phys. 10 (2001) 034; V. Balasubramanian, J. de Boer, and D. Minic, Phys. Rev. D **65**, 123508 (2002); A. M. Ghezelbash and R. B. Mann, J. High Energy Phys. 01 (2002) 005.
[3] R. B. Mann and D. Marolf, Classical Quantum Gravity **23**, 2927 (2006); D. Marolf, J. High Energy Phys. 03 (2007) 122; R. B. Mann, D. Marolf, R. McNees, and A. Virmani, Classical Quantum Gravity **25**, 225019 (2008).
[4] P. Kovtun, D. T. Son, and A. O. Starinets, Phys. Rev. Lett. **94**, 111601 (2005).
[5] S. A. Hartnoll, Classical Quantum Gravity **26**, 224002 (2009); S. A. Hartnoll, C. P. Herzog, and G. T. Horowitz, Phys. Rev. Lett. **101**, 031601 (2008); S. A. Hartnoll and P. Kovtun, Phys. Rev. D **76**, 066001 (2007); C. P. Herzog, J. Phys. A **42**, 343001 (2009).
[6] T. Faulkner, H. Liu, J. McGreevy, and D. Vegh, Phys. Rev. D **83**, 125002 (2011).
[7] J. McGreevy, Adv. High Energy Phys. **2010**, 723105 (2010).
[8] P. Hořava, Phys. Rev. D **79**, 084008 (2009).
[9] P. Koroteev and M. Libanov, J. High Energy Phys. 02 (2008) 104.
[10] S. Kachru, X. Liu, and M. Mulligan, Phys. Rev. D **78**, 106005 (2008).
[11] M. Taylor, arXiv:0812.0530.
[12] R. B. Mann, J. High Energy Phys. 06 (2009) 075.
[13] G. Bertoldi, B. A. Burrington, and A. Peet, Phys. Rev. D **80**, 126003 (2009).
[14] K. Balasubramanian and J. McGreevy, Phys. Rev. D **80**, 104039 (2009).
[15] U. H. Danielsson and L. Thorlacius, J. High Energy Phys. 03 (2009) 070.
[16] J. de Boera, M. Kulaxizia, and A. Parnachev, J. High Energy Phys. 06 (2010) 008.
[17] X. O. Camanho and J. D. Edelstein, J. High Energy Phys. 06 (2010) 099.
[18] M. H. Dehghani and R. B. Mann, J. High Energy Phys. 07 (2010) 019.
[19] E. Ayon-Beato, A. Garbarz, G. Giribet, and M. Hassaine, Phys. Rev. D **80**, 104029 (2009).
[20] E. Ayon-Beato, A. Garbarz, G. Giribet, and M. Hassaine, J. High Energy Phys. 04 (2010) 030.
[21] R. G. Cai, Y. Liu, and Y. W. Sun, J. High Energy Phys. 10 (2009) 080.
[22] D. W. Pang, J. High Energy Phys. 01 (2010) 116.
[23] M. H. Dehghani and R. B. Mann, Phys. Rev. D **82**, 064019 (2010).
[24] J. Oliva and S. Ray, Classical Quantum Gravity **27**, 225002 (2010).
[25] R. C. Myers and B. Robinson, J. High Energy Phys. 08 (2010) 067.
[26] K. Copsey and R. B. Mann, J. High Energy Phys. 03 (2011) 039.
[27] G. Dotti, J. Oliva, and R. Troncoso, Phys. Rev. D **76**, 064038 (2007).
[28] M. H. Dehghani and R. Pourhasan, Phys. Rev. D **79**, 064015 (2009).
[29] D. G. Boulware and S. Deser, Phys. Rev. Lett. **55**, 2656 (1985).
[30] R. C. Myers, M. Paulos, and A. Sinha, J. High Energy Phys. 08 (2010) 035.
[31] A. Buchel and S. Cremonini, J. High Energy Phys. 10 (2010) 026.
[32] V. Iyer and R. M. Wald, Phys. Rev. D **50**, 846 (1994).
[33] M. H. Dehghani and M. Shamirzaie, Phys. Rev. D **72**, 124015 (2005).